The Optimal Paper Moebius Band

Richard Evan Schwartz [*]

December 31, 2023

Abstract

We prove that a smooth embedded paper Moebius band must have aspect ratio greater than $\sqrt{3}$. We also prove that any sequence of smooth embedded paper Moebius bands whose aspect ratio converges to $\sqrt{3}$ must converge, up to isometry, to the famous triangular Moebius band. These results answer the mimimum aspect ratio question discussed by W. Wunderlich in 1962 and prove the more specific conjecture of B. Halpern and C. Weaver from 1977.

1   Introduction

To make a paper Moebius band you give a strip of paper an odd number of twists and then tape the ends together. For long strips this is easy and for short strips it is difficult or impossible. Figure 1 shows a famous example called the *triangular Moebius band* that is based on a $1 \times \sqrt{3}$ strip.
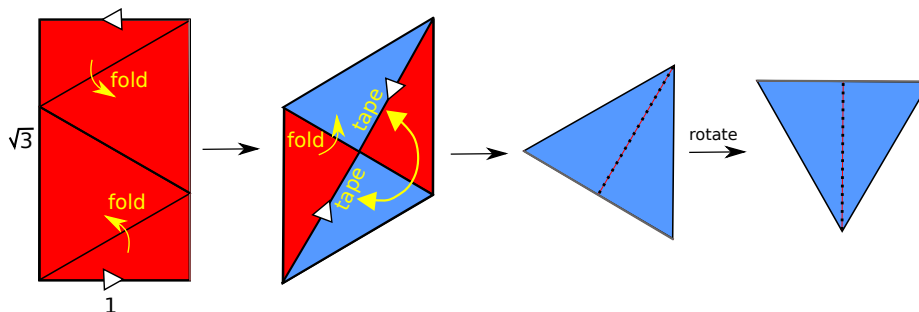
Figure 1: The triangular Moebius band

The strip in Figure 1 is colored red on one side and blue on the other. You are supposed to fold and somehow tape the thing as indicated in Figure 1. The tape runs along the dotted line in the "inside" of the little triangular "wallet" you are making. The final rotation highlights a kind of "T-pattern" made from the top edge and the dotted line, a pattern that is important in this paper. You might enjoy finding other ways of making this example in which the taping is easier to manage.

What is the smallest λ for which we can turn a $1 \times \lambda$ strip into a paper Moebius band? In order to answer this question we have to be more formal about what we are doing. Formally speaking, a *smooth paper Moebius band of aspect ratio λ* is an infinitely differentiable isometric mapping $I : M_\lambda \to \mathbf{R}^3$, where M_λ is the flat Mobius band obtained by identifying the top and bottom of a $1 \times \lambda$ rectangle. That is:

$$M_\lambda = ([0,1] \times [0,\lambda])/ \sim, \qquad (x,0) \sim (1-x,\lambda). \qquad (1)$$

An *isometric mapping* is a map which preserves arc-lengths. The map is an *embedding* if it is injective, and an *immersion* in general. The image

$$\Omega = I(M_\lambda) \qquad (2)$$

is an example of a developable surface-with-boundary. I learned about paper Moebius bands from the beautiful expository article [**FT**, Chapter 14] by Dmitry Fuchs and Sergei Tabachnikov.

The early papers of M. Sadowsky [**Sa**] and W. Wunderlich [**W**] treat both the existence and differential geometry of smooth paper Moebius bands. (See [**HF**] and [**T**] respectively for modern English translations.) The paper [**CF**] gives a modern differential geometric framework for smooth developable surfaces.

Why bother with smooth maps? Well, if you just look at ways of folding paper up to make a Moebius band you can get all kinds of weird examples. For instance, you could take a square, fold it like an accordion into a thin strip, twist, then tape. This monster is not approximable by smooth examples. The smooth formalism rules out pathologies like this. In contrast, the triangular paper Moebius band can be approximated to arbitrary precision by smooth embedded paper Moebius bands. See [**Sa**], [**HW**], and [**FT**].

W. Wunderlich discusses the minimum aspect ratio question in the introduction of his 1962 paper [**W**]. He says that it is easy to make a paper

Moebius band when $\lambda \geq 5$ and that the minimal value is not known. Since it is a very natural question I can imagine that it has been raised even earlier.

In their 1977 paper [**HW**], Halpern and Weaver study the minimum aspect ratio question in detail. They prove two things.

- For smooth immersed paper Moebius bands one has $\lambda > \pi/2$. Moreover, for any $\epsilon > 0$ one can find an immersed example with $\lambda = \pi/2 + \epsilon$.

- There exists some $\epsilon_0 > 0$ such that $\lambda > \pi/2 + \epsilon_0$ for a smooth embedded paper Moebius band. This ϵ_0 is not an explicit constant.

Halpern and Weaver give examples of smooth embedded paper Moebius bands with $\lambda = \sqrt{3} + \epsilon$ for any $\epsilon > 0$. As they point out, similar examples appear in [**Sa**]. These examples converge to the triangular Moebius band from Figure 1 as $\epsilon \to 0$. The last line of [**HW**] states the conjecture that $\lambda > \sqrt{3}$ for an embedded paper Moebius band.

In this paper I will prove the Halpern-Weaver Conjecture and show that the triangular Moebius band is uniquely the best limit.

Theorem 1.1 (Main) *A smooth embedded paper Moebius band has aspect ratio greater than $\sqrt{3}$.*

Theorem 1.2 (Triangular Limit) *Let $I_n : M_{\lambda_n} \to \Omega_n$ be a sequence of smooth embedded paper Moebius bands such that $\lambda_n \to \sqrt{3}$. Then, up to isometry, I_n converges uniformly to the triangular Moebius band map.*

Let me explain the strategy of the proofs. Let Ω be a smooth embedded paper Moebius band. A *bend* on Ω is a line segment which cuts across Ω and has its endpoints in the boundary. We say that a *T-pattern* on Ω is a pair of bends which lie in perpendicular intersecting lines. We call the T-pattern *embedded* if the two bends are disjoint. In §2.1 we prove

Lemma 1.3 (T) *A smooth embedded paper Moebius band has an embedded T-pattern.*

Our proof is topological. It is well known that Ω has a partition into continuously varying bends. We apply (essentially) the Borsuk-Ulam Theorem to a pair of functions describing the geometry of pairs of bends in this partition; the simultaneous vanishing of these functions gives us our embedded T-pattern. Our proof, slightly modified, would also show that an immersed paper Moebius band has a T-pattern.

In §2.2 we prove

Lemma 1.4 (G) *A smooth paper Moebius band with an embedded T-pattern has aspect ratio greater than $\sqrt{3}$.*

The basic idea of the proof is to cut Ω open along one of the bends comprising the T pattern and then to solve an optimization problem which involves mapping a trapezoid into space with certain constraints.

The Main Theorem is an immediate consequence of Lemma T and Lemma G. The proof of the Triangular Limit Theorem, given in §2.3, amounts to examining what our proof of Lemma G says about a minimizing sequence.

The proofs are done after §2, but I also include some more material. In §3 I will comment on the proofs and discuss some related topics. In §4, an appendix, I give a self-contained and elementary proof of the result that a smooth embedded paper Moebius band has a continuous partition into bends. I found the proofs in the literature not so easy to understand.

The ideas in this paper are an outgrowth of my earlier paper [**S1**]. In [**S1**] I prove a version of Lemma T (with some side hypotheses) and then deduce from the $t = 0$ case of Equation 4 below that $\lambda > \phi = (1 + \sqrt{5})/2$ in the embedded case. I solved an optimization problem akin to Lemma G in [**S1**] in order to further improve the bound, but I made an idiotic mistake: I thought that when you cut M_λ open along a bend you get a parallelogram rather than a trapezoid. This mistake invalidates the further bound, and all I can conclude from [**S1**] is that $\lambda > \phi$. I was amazed and delighted to discover that the correctly done optimization problem, namely Lemma G, gets the sharp bound. The work here supersedes [**S1**] and is completely independent from it.

Some readers might find this paper hard to read because I do not include much background information. I have subsequently written a longer and friendlier account [**S2**], aimed at university students and perhaps advanced high school students. This paper is available on my Brown University website. My website also has some informal notes which are even more elementary.

Here is some additional context. The topic of paper Moebius bands is adjacent to a number of different subjects. The paper [**GKS**] considers the related question of tying a piece of rope into a knot using as little rope as possible. See [**DDS**] for further results. One could view these rope knot questions as variants of the Halpern-Weaver Conjecture in a different category. Indeed, our Lemma T seems quite related in spirit to the quadrisecent idea in [**DDS**]. I will say a bit more about this in §3.2.

Paper Moebius bands are even more closely related to *folded ribbon knots*, and the triangular Moebius band can be interpreted as a folded ribbon knot. See [**D**] for a survey on this topic. More precisely, see [**DL**, Corollary 25] for a result which is in some sense a special case of our two results and see [**DL**, Conjecture 26] for a variant of the Halpern-Weaver Conjecture in the category of folded ribbon knots. I will say more about this in §3.3.

Some authors have considered "optimal Moebius bands" from other perspectives. The papers [**Sz**] considers the question from an algebraic perspective and the paper [**MK**] consider the question from a physical perspective. The paper [**SH**] precisely describes the resting shape of a paper Moebius band.

2 Proofs of the Results

2.1 Proof of Lemma T

Let $I : M_\lambda \to \Omega$ be a smooth embedded paper Moebius band. As is well known, Ω has a (not necessarily unique) partition into continuously varying bends. See §4 for a self-contained proof. We fix such a partition once and for all. We parametrize the space of bends in the partition by $\boldsymbol{R}/\lambda\boldsymbol{Z}$ as follows: We assign to each bend the point where it intersects the centerline of Ω and then, using I, we identify the centerline with $\boldsymbol{R}/\lambda\boldsymbol{Z}$.

The Cylinder: Let Υ be the topological cylinder of unequal ordered pairs $(x, y) \in (\boldsymbol{R}/\lambda\boldsymbol{Z})^2$. A point $(x, y) \in \Upsilon$ corresponds to a pair (u, v) of unequal bends. We let $\overline{\Upsilon}$ be the compactification of Υ obtained by adding 2 boundary components. The point (x, y) lies near one boundary component if y lies just ahead of x in the cyclic order coming from $\boldsymbol{R}/\lambda\boldsymbol{Z}$. The point (x, y) lies near the other boundary component if y lies just behind of x in the same cyclic order. Let $\partial\overline{\Upsilon}$ be the boundary of $\overline{\Upsilon}$. The involution $\Sigma(x, y) = (y, x)$ extends to $\overline{\Upsilon}$ and swaps the boundary components.

Oriented Bends: Let $(x, y) \in \Upsilon$ be arbitrary. There is a unique minimal path $x_t \in \boldsymbol{R}/\lambda\boldsymbol{Z}$ such that $x_0 = x$ and $x_1 = y$ and x_t is locally increasing with respect to the cyclic order on $\boldsymbol{R}/\lambda\boldsymbol{Z}$. This path is short when (x, y) is near one component of $\partial\overline{\Upsilon}$ and long near the other. Let u_t be the bend associated to x_t. Given an orientation on $u_0 = u$, we extend it continuously to an orientation on $u_1 = v$. Let $\overrightarrow{u}$ be vector parallel to our oriented u. That is, $\overrightarrow{u}$ points from the tail of u to the head of u. Likewise define $\overrightarrow{v}$. We write $\overrightarrow{u} \rightsquigarrow \overrightarrow{v}$. Since we are on a Moebius band, $\overrightarrow{v} \rightsquigarrow -\overrightarrow{u}$.

The Functions: Let m_u and m_v be the midpoints of u and v. Define

$$g(x, y) = \overrightarrow{u} \cdot \overrightarrow{v}, \qquad h(x, y) = (m_u - m_v) \cdot (\overrightarrow{u} \times \overrightarrow{v}). \tag{3}$$

If we had started with the other orientation of u we would get the same value for g and h because $-\overrightarrow{u} \rightsquigarrow -\overrightarrow{v}$. Hence g and h are well defined. Note that g and h extend continuously to $\overline{\Upsilon}$. Note the following:

1. On one component of $\partial\overline{\Upsilon}$ we have $g \geq 1$ and $h = 0$.

2. On the other component of $\partial\overline{\Upsilon}$ we have $g \leq -1$ and $h = 0$.

3. We have $g \circ \Sigma = -g$ and $h \circ \Sigma = -h$.

Here is the justification for Claim 3.

$$g(y, x) = \overrightarrow{v} \cdot (-\overrightarrow{u}) = -g(x, y).$$

$$h(y, x) = (m_v - m_u) \cdot (\overrightarrow{v} \times (-\overrightarrow{u})) = (m_v - m_u) \cdot (\overrightarrow{u} \times \overrightarrow{v}) = -h(x, y).$$

Lemma 2.1 *If $g(x, y) = h(x, y) = 0$ then (u, v) is an embedded T-pattern.*

Proof: Since $g(x, y) = 0$ the vectors $\overrightarrow{u}$ and $\overrightarrow{v}$ are orthogonal. Hence $\overrightarrow{n} = \overrightarrow{u} \times \overrightarrow{v}$ is nonzero. By construction u and v and the segment $\overline{m_u m_v}$ all lie in planes orthogonal to $\overrightarrow{n}$. Since $u \cup v \cup \overline{m_u m_v}$ is connected, this union lies in the same plane orthogonal to $\overrightarrow{n}$. In short, u and v are co-planar. The bends are disjoint because they are in the same partition. ♠

To prove Lemma T, we just have to prove that g and h simultaneously vanish somewhere in Υ. Suppose not. Since $|g| \geq 1$ on $\partial \overline{\Upsilon}$, we can say that g and h do not simultaneously vanish on $\overline{\Upsilon}$. Let S^1 be the unit circle. Let $A = (g, h)$ and $B = A/\|A\|$. Then $B : \overline{\Upsilon} \to S^1$ is well-defined and continuous. B maps one component of $\partial \overline{\Upsilon}$ to $(1, 0)$ and the other to $(-1, 0)$.

Consider a path γ which connects a point in one component of $\partial \overline{\Upsilon}$ to a point in the other. The image $B(\gamma)$, when oriented from $(1, 0)$ to $(-1, 0)$, winds some half integer $w(\gamma)$ times around the origin. All choices of γ are homotopic to each other relative to $\partial \overline{\Upsilon}$. Thus $w(\gamma)$ is independent of γ. In particular, $w(\Sigma(\gamma)) = w(\gamma)$. However, $B \circ \Sigma = -B$. So, when we orient $B(\Sigma(\gamma)) = -B(\gamma)$ from $(1, 0)$ to $(-1, 0)$, as illustrated in Figure 2, the winding number is $-w(\gamma)$. This contradiction completes the proof.
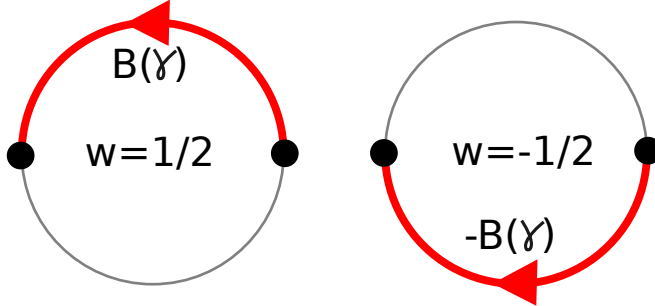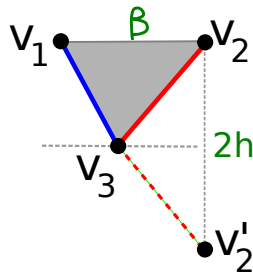

Figure 2: The effect of negation: a cartoon

2.2   Proof of Lemma G

Let ∇ be a triangle with horizontal base. Let $p(\nabla)$ be the perimeter of ∇ and let $n(\nabla)$ be the sum of the lengths of the non-horizontal edges of ∇.

Lemma 2.2 *If ∇ has base $\sqrt{1+t^2}$ and height $h \geq 1$ then $n(\nabla) \geq \sqrt{5+t^2}$ and $p(\nabla) \geq \sqrt{1+t^2} + \sqrt{5+t^2}$. Equality occurs iff ∇ is isosceles and $h = 1$.*

Proof: This is an extremely well known kind of result. Let $\beta = \sqrt{1+t^2}$.

Figure 3: The diagram for Lemma 2.2.

Let v_1, v_2, v_3 be the vertices of ∇, with v_3 the apex. Let v_2' be the reflection of v_2 through the horizontal line containing v_3. By symmetry, the triangle inequality, and the Pythagorean Theorem,

$$n(\nabla) = \|v_1 - v_3\| + \|v_3 - v_2'\| \geq \|v_1 - v_2'\| = \sqrt{\beta^2 + 4h^2} \geq \sqrt{\beta^2 + 4} = \sqrt{5+t^2}.$$

The bound for $p(\nabla)$ follows immediately. In the case of Equality, $h = 1$ and v_1, v_3, v_2' are collinear, meaning that ∇ is isosceles. ♠

Let $I : M_\lambda \to \Omega$ be a paper Moebius band with an embedded T-pattern. We write $S' = I(S)$ for any relevant set S and we let $\ell(\cdot)$ denote arc-length. By definition, we have $\ell(\gamma) = \ell(\gamma')$ for any curve $\gamma \subset M_\lambda$. For instance, $\ell(\partial M_\lambda) = \ell(\partial \Omega)$.

Let B' and T' be the pair of disjoint bends comprising an embedded T-pattern of Ω. Since they lie on intersecting lines, B' and T' are co-planar. We choose so that the line extending T' is disjoint from B', then rotate so that B' and T' are respectively vertical and horizontal segments in the XY-plane and B' is strictly below the line extending T'. Let B and T be the line segments on M_λ corresponding to B' and T'. We cut M_λ open along B to get a bilaterally symmetric **trapezoid**. See Figure 4.
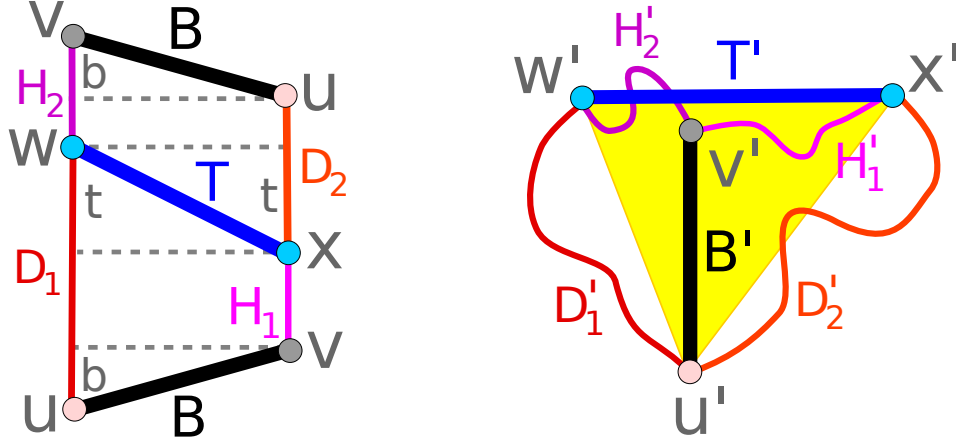
Figure 4: The trapezoid (left) and the T-pattern (right).

Here $-t$ is the slope of T. The quantity b, which is the slope of the bottom choice of B, plays no role in our calculations. The picture looks a bit different when the signs of t and b are different, but it is always true that $\ell(H_1) + \ell(H_2) = \ell(D_1) + \ell(D_2) - 2t$. The yellow triangle ∇ has base $\sqrt{1+t^2}$ and height greater than 1.

First Bound: We have $2\lambda > \sqrt{1+t^2} + \sqrt{5+t^2}$. Here is the derivation:

$$2\lambda = \ell(\partial M_\lambda) = \ell(\partial \Omega) \geq p(\nabla) > \sqrt{1+t^2} + \sqrt{5+t^2}. \tag{4}$$

The first inequality comes from the fact that $\partial \Omega$ is a (red and magenta) loop containing all vertices of ∇. The second inequality is Lemma 2.2.

Second Bound: We have $2\lambda > 2\sqrt{5+t^2} - 2t$. Here is the derivation.

$$2\lambda = \ell(D_1) + \ell(D_2) + \ell(H_1) + \ell(H_2) = 2\ell(D_1) + 2\ell(D_2) - 2t =$$

$$2\ell(D_1') + 2\ell(D_2') - 2t \geq 2n(\nabla) - 2t > 2\sqrt{5+t^2} - 2t. \tag{5}$$

The first inequality comes from the fact that $D_1' \cup D_2'$ is a (red) path that connects w' to x' and contains u'. The second inequality is Lemma 2.2.

Combining the Bounds: Let $t_0 = 1/\sqrt{3}$. If $t \geq t_0$ then our first bound gives $\lambda > \sqrt{3}$. If $t \leq t_0$ then our second bound gives $\lambda > \sqrt{3}$. Hence $\lambda > \sqrt{3}$. This completes the proof of Lemma G.

9

2.3 Proof of the Triangular Limit Theorem

Suppose we have a sequence $\{\Omega_n\}$ of embedded paper Moebius bands with $\lambda_n \to \sqrt{3}$. We run the constructions from Lemma G for each one. Looking at the analysis done at the end of the proof of Lemma G, we see that

$$t_n \to t_0 = 1/\sqrt{3}.$$

Also $b_n \to 0$, because otherwise the height of ∇_n, which exceeds $\sqrt{1 + b_n^2}$, does not converge to 1. The parameters $b = 0$ and $t = 1/\sqrt{3}$ respectively describe the top/bottom bend B' and the middle bend T' shown on the red strip in Figure 1 (left). We normalize by isometries of M_{λ_n} so that $B'_n \to B'$ and $T'_n \to T'$.

Thanks to the uniqueness in Lemma 2.2, the triangle ∇_n converges up to isometry to the equilateral triangle ∇ of perimeter $2\sqrt{3}$ shown in Figure 1 (right). We normalize by isometries of $\boldsymbol{R}^3$ so that the vertices of ∇_n converge to the vertices of ∇. Inspecting Equation 4, we see that

$$|\ell(\partial\Omega_n) - p(\nabla)| \to 0. \tag{6}$$

Since I_n is length perserving the convergence in Equation 6 implies that I_n, when restricted to each of the 4 segments $D_{n,j}$ and $H_{j,n}$ in ∂M_{λ_n}, converges uniformly to a linear isometry. Hence the restriction of I_n to ∂M_{λ_n} converges uniformly to the map that comes from the triangular Moebius band. The action of I_n on ∂M_{λ_n} determines the action of I_n on M_{λ_n}, so the convergence on the boundary implies the convergence on the whole space. This completes the proof of the Triangular Limit Theorem.

3   Discussion

3.1   Lemma G

The proof of Lemma G only requires the map $I : M_\lambda \to \Omega$ to have the following properties.

1. I is continuous.

2. The interior of M_λ has a continuous partition by open line segments whose endpoints lie in the boundary.

3. Given an arbitrary line segment v in the partition the image $I(v)$ is a line segment in $\boldsymbol{R}^3$ that is at least as long as v.

4. The restriction $I : \partial M_\lambda \to \partial \Omega$ never increases arc-length.

5. There exist 2 segments v, w in the partition and a linear projection ϕ onto a plane such that $\phi \circ I$ is distance non-decreasing on each of v and w and such that $\phi \circ I(v)$ and $\phi \circ I(w)$ are disjoint and perpendicular.

The Triangular Limit Theorem does not quite work in this generality, because the restriction of I to ∂M_λ does not determine the action of I on all of M_λ. Nevertheless, we can say that for a minimizing sequence $\{I_n\}$, the maps converge uniformly on the boundary, up to isometry, to the triangular Moebius band map. Also, up to isometries the images Ω_n converge (e.g. in the Hausdorff metric) to the triangular paper Moebius band.

3.2   Lemma T

Borsuk-Ulam Theorem: The proof I give of Lemma T is quite close to a proof of the Borsuk-Ulam Theorem. Indeed, Jeremy Kahn pointed out to me that the endgame of my proof really is the Borsuk-Ulam proof in disguise. To see this, note that we obtain the 2-sphere S^2 by crushing each component of $\partial \overline{\Upsilon}$ to a point. Then B induces a map $S^2 \to S^1$ with $B \circ \Sigma = -B$. The map Σ, which is a glide reflection on $\overline{\Upsilon}$, acts on S^2 as the antipodal map.

There is a very nice way to do all this explicitly. We think of $\overline{\Upsilon}$ as the set of equivalence classes of points $(x, y) \in \boldsymbol{R}^2$ such that $x \leq y \leq x + 1$. The equivalence relation is $(x, y) \sim (x + k, y + k)$ for all $k \in \boldsymbol{Z}$. Here is a

continuous surjection from $\overline{\Upsilon}$ to S^2 which maps the boundary components to $(0, 0, \pm 1)$ and is a homeomorphism from Υ to $S^2 - \{(0, 0, \pm 1)\}$:

$$(x, y) \rightarrow (\sqrt{1 - z^2} \cos(\theta), \sqrt{1 - z^2} \sin(\theta), z),$$

$$\theta = \pi(x + y), \qquad z = 2x - 2y + 1. \tag{7}$$

The action of Σ on this version of Υ maps the class of (x, y) to the class of $(y, x + 1)$. The map in Equation 7 respects the equivalence relation and conjugates Σ to the antipodal map.

We now redefine the vectors $\overrightarrow{u}$ and $\overrightarrow{v}$ to be the *unit vectors* parallel to the orientations of u and v. Once this is done, the functions g and h themselves extend to S^2 and satisfy $g(-P) = -g(P)$ and $h(-P) = -h(P)$ for all $P \in S^2$. We then conclude from the Borsuk-Ulam Theorem that there is some $P \in S^2$ such that $g(P) = h(P) = 0$. Since $g((0, 0, \pm 1)) = \pm 1$ we conclude that $P \neq (0, 0, \pm 1)$. Hence P actually corresponds to a T-pattern.

Paths of Oriented Lines: Anton Izosimov and Sergei Tabachnikov independently suggested to me the following formulation of Lemma T.

Lemma 3.1 *Suppose $\{L_t | \ t \in [0, 1]\}$ is a continuous family of oriented lines in $\mathbf{R}^3$ such that $L_1 = L_0^{\mathrm{opp}}$, the same line as L_0 but with the opposite orientation. Then there exist parameters $r, s \in [0, 1]$ such that L_r and L_s are perpendicular intersecting lines.*

This result immediately implies Lemma T, and it has essentially the same proof. In particular, Lemma 3.1 applies to maps $I : M_\lambda \rightarrow \Omega$ which satisfy Conditions 1-4 above. The output is a T-pattern which might or might not be embedded. If I is an embedding then, of course, the T-pattern will also be embedded.

The Study Sphere: Sergei also suggested to me a beautiful alternate formalism for the proof of Lemma T. One introduces the *Study numbers*. These have the form $x + \epsilon y$ where $x, y \in \mathbf{R}$ and $\epsilon^2 = 0$. Likewise, one introduces the *Study vectors*. These have the form $\overrightarrow{a} + \epsilon \overrightarrow{b}$, where $\overrightarrow{a}, \overrightarrow{b} \in \mathbf{R}^3$ and again $\epsilon^2 = 0$. In this context, the dot product of two Study vectors makes sense and is a Study number.

Each oriented line $\ell \subset \mathbf{R}^3$ gives rise to a Study vector $\xi_\ell = \overrightarrow{a} + \epsilon \overrightarrow{b}$ where $\overrightarrow{a}$ is the unit vector pointing in the direction of ℓ and $\overrightarrow{b} = \ell' \times \overrightarrow{a}$. Here

$\ell' \in \ell$ is any point. All choices of ℓ' give rise to the same $\overrightarrow{b}$; this vector is called the *moment vector* of ℓ. This formalism identifies the space of oriented lines in $\boldsymbol{R}^3$ with the so-called *study sphere* consisting of Study vectors ξ such that $\xi \cdot \xi = 1$. The Study dot product $\xi_\ell \cdot \xi_m$ vanishes if and only if ℓ and m are perpendicular and intersect. Thus our two functions g and h carry the same information as the Study dot product. This makes the functions g and h seem more canonical.

Quadruple Point Configurations: After proving the Halpern-Weaver Conjecture, I heard from a number of people who asked me how I thought of Lemma T. I can't remember exactly, but here is one association. Around the time I got interested in the Halpern-Weaver Conjecture I had been thinking quite a bit about the Square Peg Conjecture. (I often think about this conjecture.) This conjecture, which goes back to Toeplitz in 1911, asks if every continuous loop in the plane contains 4 points which make the vertices of a square. See [**Mat**] for a fairly recent survey of work done on it. One can view a T-pattern as a collection of 4 points in the boundary of the Moebius band which satisfy certain additional constraints – e.g. they are coplanar. Put this way, a T-pattern does not seem so different from a square inscribed in a Jordan loop.

As I mentioned in the introduction, the idea for Lemma T is also similar in spirit for the idea developed in [**DDS**] concerning 4 collinear points on a knotted loop. These so-called *quadrisecants* play a role similar to Lemma T in getting a lower bound for the length of a knotted rope. I wasn't thinking about this at the time, however.

3.3   Folded Ribbon Knots

Elizabeth Denne pointed out to me the connection between paper Moebius bands and *folded ribbon knots*. Her paper with Troy Larsen [**DL**] gives a formal definition of a folded ribbon knot and has a wealth of interesting constructions, results, and conjectures. See also her survey article [**D**].

Informally, folded ribbon knots are the objects you get when you take a flat cylinder or Moebius band, fold it into a knot, and then press it into the plane. Associated to a folded ribbon knot is a polygon, which comes from the centerline of the object. Even though the ribbon knot lies entirely in the plane, one assigns additional combinatorial data which keeps track of "infinitesimal" under and over crossings as in a knot diagram. So the

associated centerline is really a knot (or possibly the unknot).

[**DL**, Corollary 25] proves our Main Theorem in the category folded ribbon Moebius bands whose associated polygonal knot is a triangle. This is a finite dimensional problem. [**DL**, Conjecture 26] says that [**DL**, Corollary 25] is true without the restriction that the associated polygonal knot is a triangle, and this is an infinite dimensional problem like the Halpern-Weaver Conjecture.

The combination of our Main Theorem and the Triangular Limit Theorem implies [**DL**, Conjecture 26]. One takes arbitrarily nearby smooth approximations, as in [**HW**], and then applies our results to them. Alteriatively, the same proof that we gave of Lemmas G and T probably would work in this category. (I did not think this through in all details.)

One might also ask about the converse. If it were possible to flatten, through isometric embeddings, an arbitrary paper Moebius band into a knotted ribbon graph, then [**DL**, Conjecture 26] would imply our results. (Again, I did not think this through in all details.) While I do not think that all twisted paper Moebius bands have this property, it might be the case that paper Moebius bands with sufficiently small aspect ratio do have this property. In any case, the possibility of flattening paper Moebius bands isometrically into folded ribbon knots seems like an appealing topic for further investigation.

3.4   More Twists

The Halpern-Weaver Conjecture is one of infinitely many similar kinds of questions one can ask about paper Moebius bands. For instance, one can take essentially all the many conjectures made in [**DL**] and translate them from the language of folded ribbon knots to the language of paper Moebius bands. Let me discuss the extent to which I have thought about this.

Twisted Cylinders: One can make a *twisted cylinder* by taking a $1 \times \lambda$ strip of paper, giving it an even and nonzero number of twists, and then taping the ends together. Such an object has a formal definition similar to what I gave for paper Moebius bands. The essential feature of twisted cylinders is that their two boundary components make a nontrivial link. As for the case of paper Moebius bands, there are optimal limiting shapes which have interpretations as folded ribbon knots.

Unlike the case considered in this paper, there are two distinct limiting

folding patterns. Both of them are folding patterns which wrap a 1×2 strip 4 times around a right-angled isosceles triangle. In [**S3**] I prove that a twisted cylinder has aspect ratio greater than 2 and that any minimizing sequence converges on a subsequence to one of the two optimal models. This result also confirms the $n = 1$ case of [**DL**, Conjecture 39]. The proof is somewhat similar to what I do in this paper, though the fine-scale details are different. Noah Montgomery independently came up with a proof of the cylinder result. His elegant proof is different than mine.

Multi-Twisted Moebius bands: We define a *multi-twisted paper Moebius band* to be what you get when you take a $1 \times \lambda$ strip of paper and give it an odd number of at least 3 twists. An essential feature of these objects is that their boundaries are knotted. I think it follows from the Triangular Limit Theorem and from compactness that there is some ϵ_0 such that the aspect ratio of a multi-twisted paper Moebius band is at least $\sqrt{3} + \epsilon_0$.

Brienne Brown did some experiments with these objects and found two candidate optimal models. We call these the *crisscross* and the *cup*. Both are made from a 1×3 strip of paper. The crisscross is planar, and has an interpretation as a folded ribbon knot. The cup is not-planar: It is a double wrap of 3 mutually orthogonal right-angled isoceles triangles arranged like 3 faces of a tetrahedron. We wrote about this in [**BS**], and conjecture there that $\lambda > 3$ for an embedded multi-twisted paper Moebius band. The non-planar nature of the cup makes me think that the kind of proofs I give in this paper, which are essentially planar arguments, will not be able to establish this conjecture. Some new ideas are needed.

One can define an n-twisted paper strip in the obvious way. When n is odd, these are paper Moebius bands and when n is even these are paper cylinders. Let λ_n be the infimal value of aspect ratios of n-twist embedded paper strips. Our Main Theorem combines with the result in [**HW**] to say that $\lambda_1 = \sqrt{3}$. The results in [**S3**] say that $\lambda_2 = 2$. We conjecture in [**BS**] that $\lambda_3 = 3$. Noah Montgomery has a construction showing that λ_n grows at most like $\sqrt{n}$. Recently, Aidan Hennessey showed me a construction which seems to prove that $\lambda_n < 8$ for all n.

4 Appendix: The Bend Partition

4.1 The Proof Modulo a Detail

Let Ω be a smooth embedded paper Moebius band. Recall that a *bend* is a straight line segment on Ω having its endpoints in $\partial\Omega$. For the convenience of the reader, I will give a self-contained proof of the following result.

Theorem 4.1 *There is a continuous partition of Ω into bends.*

Let Ω^o be the interior of Ω. Let S^2 be the unit 2-sphere. The *Gauss map*, which is well defined and smooth on any simply-connected subset Ω^o, associates to each point $p \in \Omega^o$ a unit normal vector $n_p \in S^2$. Let dn_p be the differential of the Gauss map at p. Since the curvature Ω^o is 0 everywhere, dn_p has a nontrivial kernel. The point p has nonzero *mean curvature* if and only if dn_p has nontrivial image. Let $U \subset \Omega^o$ denote the subset having nonzero mean curvature. Theorem 4.1 is a quick consequence of the following result in differential geometry.

Lemma 4.2 *Each $p \in U$ lies in a unique bend γ. Furthermore, the interior of γ lies in U.*

Lemma 4.2 is a special case of the two essentially identical results, [**CL**, p. 314, Lemma 2] and [**HN**, §3, Lemma 2]. These results and proofs are done in a general multi-dimensional setting. Below I give an elementary and geometric proof tailored to the 2-dimensional case.

It follows immediately from Lemma 4.2 that U has a continuous partition into bends. The uniqueness implies the continuity. Let τ be a component of $\Omega - U$. If τ has empty interior then τ is a line segment, the limit of a sequence of bends. In this case τ is also a bend. Suppose τ has non-empty interior. The Gauss map is constant on τ and hence τ lies in a single plane. Two sides of τ, opposite sides, lie in $\partial\Omega$ and are straight line segments. The other two sides of τ, the other opposite sides, are bends. Thus τ is a planar trapezoid. But then we can extend our bend partition across τ by simply choosing any continuous family of segments on τ that interpolates between the two bends in its boundary. Indeed, there is a canonical extension: If the two bends of $\partial\tau$ lie on parallel lines we can take the interpolating bends to lie on parallel lines. If they lie on intersecting lines, we can take the interpolating bends to lie on lines which all go through the intersection point. Doing this construction on all such components, we get our continuous partition of Ω into bends.

4.2   Proof of Lemma 4.2

Let $U \subset \Omega^o$ as above. Let $p \to n_p$ be a local choice of the Gauss map. We can rotate and translate so that near the origin U is the graph of a function

$$F(x, y) = Cy^2 + \text{higher order terms.} \tag{8}$$

Here $C > 0$ is some constant. The normal vector at the origin is $n_0 = (0, 0, 1)$. The vector $v_0 = (1, 0, 0)$ lies in the kernel of dn_0. Let $w_0 = (0, 1, 0)$. Let Π_0 be the plane spanned by w_0 and n_0. The image of $\Pi_0 \cap U$ under the Gauss map is (near n_0) a smooth regular curve tangent to w_0 at n_0. The sign depends on the choice of local Gauss map.

Working locally, we have three smooth vectorfields:

$$p \to n_p, \qquad p \to v_p, \qquad p \to w_p = v_p \times n_p. \tag{9}$$

Here v_p is the kernel of dn_p and $\times$ denote the cross product. Let Π_p be the plane through p and spanned by w_p and n_p. From our analysis of the special case, and from symmetry, the image of $\Pi_p \cap U$ under the Gauss map is (near n_p) a smooth regular curve tangent to w_p at n_p. The *asymptotic curves* are the smooth curves everywhere tangent to the v vector field.

Lemma 4.3 *The asymptotic curves are line segments.*

Proof: Let γ be an asymptotic curve. By construction, the Gauss map is constant along γ. About each point in γ there is a small neighborhood V which is partitioned into asymptotic curves that transversely intersect each plane Π_p when $p \in \gamma \cap V$. Hence the image of V under the Gauss map equals the image of $\Pi_p \cap V$ under the Gauss map. This latter image is a smooth regular curve tangent to w_p at n_p. Since this is true for all $p \in \gamma \cap V$ and since n_p is constant along γ we see that w_p is constant along γ. Hence v_p is constant along γ. Hence γ is a line segment. ♠

The nonzero mean curvature implies that γ is the unique line segment through any of its interior points. We just have to rule out the possibility that γ reaches ∂U before it reaches $\partial \Omega$. Assume for the sake of contradiction that this happens. We normalize as in Equation 8.

We now allow ourselves the liberty of dilating our surface. This dilation preserves all the properties we have discussed above. By focusing on a point of γ sufficiently close to ∂U and dilating, we arrange the following:

- A neighborhood $\mathcal{V}$ of Ω^o is the graph of a function over the disk of radius 3 centered at the origin.

- Given $p \in \mathcal{V}$ let p' be the projection of p to the XY-plane. We have $|p'_1 - p'_2| > (2/3)|p_1 - p_2|$ for all $p_1, p_2 \in \mathcal{V}$.

- $\gamma \subset U$ contains the arc connecting $(0,0,0)$ to $(3,0,0)$, but $(0,0,0) \notin U$.

Let $a \in (0,3)$. At $(a,0,0)$ we have $v_a = (1,0,0)$ and $w_a = (0,1,0)$ and $n_a = (0,0,1)$. Let Π_a be the plane $\{X = a\}$. Near $(a,0,0)$, the intersection $U_a = U \cap \Pi_a$ is a smooth curve tangent to w_a at $(a,0,0)$.

Let $\zeta = (1,0,0)$. Fix $\delta > 0$. By continuity and compactness, the asymptotic curves through points of U_1 sufficiently near ζ contain line segments connecting points on U_2 to points on U_δ. Call these *connectors*. There exists a canonical map $\Phi_\delta : U_1 \to U_\delta$ defined in a neighborhood of ζ: The points $q \in U_1$ and $\Phi_\delta(q) \in U_\delta$ lie in the same connector.

Lemma 4.4 Φ_δ *expands distances by less than a factor of* 3.

Proof: Let ℓ_1 and ℓ_2 be two connectors. Let $a_j = \ell_j \cap U_1$. Let $b_j = \ell_j \cap U_\delta$. For any set S let S' be the projection of S to $\boldsymbol{R}^2$. We have the bounds

$$\frac{|a'_1 - a'_2|}{|a_1 - a_2|}, \frac{|b'_1 - b'_2|}{|b_1 - b_2|} \in \left[\frac{2}{3}, 1\right], \qquad \frac{|a'_j - b'_j|}{\text{length}(\ell'_j)} < 2.$$

Geometrically, a'_j is very nearly the midpoint of ℓ'_j and b'_j is the closer of the two endpoints. Since ℓ'_1 and ℓ'_2 are planar and disjoint, our last inequality (and essentially a similar-triangles argument) gives $|b'_1 - b'_2|/|a'_1 - a'_2| < 2$. Putting everything together, we have $|b_1 - b_2|/|a_1 - a_2| < 3$. ♠

Fix $\epsilon > 0$. The mean curvature along U_δ tends to 0 as $\delta \to 0$. If we choose δ sufficiently small then the Gauss map expands distances along U_δ in a neighborhood of $(\delta, 0, 0)$ by a factor of less than ϵ. Combining Lemma 4.4 and the fact that $n_q = n_{\Phi_\delta(q)}$, we see that the Gauss map expands distances by at most a factor of 3ϵ along U_1 in a small neighborhood of ζ. Since ϵ is arbitrary, $w_1 \in \ker(dn_\zeta)$. But $v_1 \in \ker(dn_\zeta)$ by definition. Hence dn_ζ is the trivial map. The contradicts the fact that $\zeta \in U$.

This completes the proof of Lemma 4.2.

5　References

[**BS**] B. E. Brown and R. E. Schwartz, *The crisscross and the cup: Two short 3-twist paper Moebius bands*, preprint 2023, arXiv:2310.10000

[**CF**] Y. Chen and E. Fried, *Mobius bands, unstretchable material sheets and developable surfaces*, Proceedings of the Royal Society A, (2016)

[**CKS**] J. Cantarella, R. Kusner, J. Sullivan, *On the minimum ropelength of knots and links*, Invent. Math. **150** (2) pp 257-286 (2003)

[**CL**], S.-S. Chern and R. K. Lashof, *On the total curvature of immersed manifolds*, Amer. J. Math. **79** (1957) pp 306–318

[**D**] E. Denne, *Folded Ribbon Knots in the Plane*, The Encyclopedia of Knot Theory (ed. Colin Adams, Erica Flapan, Allison Henrich, Louis H. Kauffman, Lewis D. Ludwig, Sam Nelson) Chapter 88, CRC Press (2021)

[**DL**] E. Denne, T. Larsen, *Linking number and folded ribbon unknots*, Journal of Knot Theory and Its Ramifications, Vol. 32 No. 1 (2023)

[**DDS**] E. Denne, Y. Diao, J. M. Sullivan, *Quaadrisecants give new lower bounds for the ropelength of a knot*, Geometry&Topology 19 (2006) pp 1–26

[**FT**], D. Fuchs, S. Tabachnikov, *Mathematical Omnibus: Thirty Lectures on Classic Mathematics*, AMS 2007

[**HF**], D.F. Hinz, E. Fried, *Translation of Michael Sadowsky's paper 'An elementary proof for the existence of a developable MÖBIUS band and the attribution of the geometric problem to a variational problem'*. J. Elast. 119, 3–6 (2015)

[**HL**], P. Hartman and L. Nirenberg, *On spherical maps whose Jacobians do not change sign*, Amer. J. Math. **81** (1959) pp 901–920

[**HW**], B. Halpern and C. Weaver, *Inverting a cylinder through isometric immersions and embeddings*, Trans. Am. Math. Soc **230**, pp 41–70 (1977)

[**MK**] L. Mahadevan and J. B. Keller, *The shape of a Möbius band*, Proceedings of the Royal Society A (1993)

[**Ma1**] B. Matschke, *A survey on the Square Peg Problem*, Notices of the A.M.S. **Vol 61.4**, April 2014, pp 346-351.

[**Sa**], M. Sadowski, *Ein elementarer Beweis für die Existenz eines abwickelbaren MÖBIUSschen Bandes und die Zurückführung des geometrischen Problems auf einVariationsproblem*. Sitzungsberichte der Preussischen Akad. der Wissenschaften, physikalisch-mathematische Klasse 22, 412–415.2 (1930)

[**S1**] R. E. Schwartz, *An improved bound on the optimal paper Moebius band*, Geometriae Dedicata, 2021

[**S2**] R. E. Schwartz, *The Optimal Paper Moebius Band: A Friendly Account*, preprint, 2023

[**S3**] R. E. Schwartz, *The Optimal Twisted Paper Cylinder*, preprint 2023, arXiv:2309.14033

[**SH**] E. L. Starostin, G. H. M. van der Heijden, *The shape of a Möbius Strip*, Nature Materials **6** (2007) pp 563 – 567

[**Sz**] G. Schwarz, *A pretender to the title "canonical Moebius strip"*, Pacific J. of Math., **143** (1) pp. 195-200, (1990)

[**T**] Todres, R. E., *Translation of W. Wunderlich's On a Developable Möbius band*, Journal of Elasticity **119** pp 23–34 (2015)

[**W**] W. Wunderlich, *Über ein abwickelbares Möbiusband*, Monatshefte für Mathematik **66** pp 276–289 (1962)